Electronic Supplementary Material

Yb- and Er concentration dependence of the upconversion luminescence of highly doped $NaYF_4$:Yb,Er/$NaYF_4$:Lu core/shell nanocrystals prepared by a water-free synthesis

Christian Würth[1], Bettina Grauel[1], Monika Pons[1], Florian Frenzel[1], Philipp Rissiek[2], Kerstin Rücker[1], Markus Haase[1] (✉), and Ute Resch-Genger[1] (✉)

[1] *Federal Institute for Materials Research and Testing (BAM), Division Biophotonics, Richard-Willstaetter-Str. 11, 12489 Berlin, Germany*
[2] *Institut für Chemie Neuer Materialien, Fachbereich Biologie/Chemie, Universität Osnabrück, Barbarastraße 7, 49076 Osnabrück, Germany*

Supporting information to https://doi.org/10.1007/s12274-022-4570-5

Materials and Methods

Reagents

Oleic acid (purified, Fisher Scientific), 1-octadecene (technical grade 90 %, Alfa Aesar), ammonium fluoride (min. 98.0 %, Alfa Aesar), sodium oleate (82 %, Sigma Aldrich), acetic acid (99.5 %, Grüssing), acetic anhydride (Ph. Eur., VWR), yttrium oxide (99.9 %, Intematix), ytterbium oxide and erbium oxide (99.9 %, Chemos), lutetium oxide (99.99% Alfa Aesar). All materials were used as received. Anhydrous rare earth acetates were prepared as previously reported. [1]

α-Na_xYF_{3+x}:Yb,Er precursor particles for β-*$NaYF_4$:Yb,Er core particles:*

First, 300 ml of oleic acid and 300 ml of 1-octadecene were loaded in a 1000 ml three neck round bottom flask. The flask was connected to a Schlenk-line and the solvents dried at 100 °C by applying vacuum (< 0.1 mbar) for one hour. After switching to nitrogen atmosphere, in total 30 mmol of anhydrous yttrium acetate, ytterbium acetate, and erbium acetate (see table below), were added at 100 °C. The flask was placed under vacuum again and further heated at 100 °C until the precursors were fully dissolved, and the evolution of gas came to an end (~75 min). The reaction vessel was then backfilled with nitrogen and heated to 300°C to further release acetic acid. After 10 minutes at 300 °C, the heating mantle was removed and the solution was left under nitrogen atmosphere to cool naturally to 100 °C. Vacuum was again applied for 60 minutes to remove the acetic acid released. Then, the flask was again backfilled with nitrogen and sodium oleate were added at 100 °C under weak nitrogen flow. The amount of sodium oleate was varied, as given in the table below, to control the number of β-phase seeds and obtain particles of similar size for all dopant concentrations. [2,3] Vacuum was again applied and the sodium oleate was dissolved by stirring the suspension for 30 minutes at 100 °C. After this dissolution and degassing step, the stoichiometric amount of solid NH_4F was added at 100 °C under weak nitrogen flow (see table 1). In order to remove air, the reaction vessel was subjected three times to a short vacuum (3-5 sec.) and backfilled with nitrogen. Then, the mixture was heated to 200 °C and kept at this temperature for 1 h. Thereafter, the heating mantle was removed. After the solution had cooled naturally to a temperature below 40 °C, the NaF formed as by-product was removed by centrifugation. The nanoparticles were precipitated from the supernatant by adding 600 ml of ethanol and were subsequently separated by centrifugation. For further purification, the precipitate was redispersed in 60 ml of hexane and precipitated again with 60 ml of ethanol. The precipitate was isolated by centrifugation and redispersed in 60 ml of hexane. The clear solution was tightly closed and stored in a refrigerator at approximately 6 °C.

Address correspondence to Markus Haase, markus.haase@uni-osnabrueck.de; Ute Resch-Genger, ute.resch@bam.de

TSINGHUA UNIVERSITY PRESS Springer

α-$NaYF_4$:Yb,Er	$Y(OAc)_3$ / mmol	$Yb(OAc)_3$ / mmol	$Er(OAc)_3$ / mmol	NaOAc / mmol	NH_4F/ mmol
20% Yb, 2% Er	23,4	6	0,6	75	165
40% Yb, 2% Er	17,4	12	0,6	75	165
60% Yb, 2% Er	11,4	18	0,6	120	210
98% Yb, 2% Er	0	29,4	0,6	120	210
60% Yb, 10% Er	9	18	3	75	165
60% Yb, 20% Er	6	18	6	75	165
60% Yb, 40% Er	0	11,8	18,3	75	165

α-Na_xYF_{3+x}:Lu precursor particles for the β-$NaYF_4$:Lu shell:

In an analogous way, small α-Na_xYF_{3+x}:Lu particles were prepared as shell precursor. In this case, a total amount of 30 mmol of yttrium acetate and lutetium acetate was dissolved in 300 ml oleic acid and 300 ml 1-octadecene and combined with sodium oleate and solid NH_4F as given in the table below. In the synthesis, a low molar ratio of rare earth acetates to sodium acetate of only 1.5 was used to avoid the formation of β-$NaYF_4$:Lu particles in the subsequent core/shell synthesis.[3] As above, the final product (30 mmol of precursor particles) was redispersed in 60 ml of hexane and the clear solution stored in a refrigerator at approximately 6 °C.

α-$NaYF_4$:Lu	$Y(OAc)_3$ / mmol	$Lu(OAc)_3$ / mmol	NaOAc / mmol	NH_4F/ mmol
22% Lu	23,4	6,6	45	135
42% Lu	16,68	13,15	45	135
62% Lu	11,4	18,6	45	135
100%Lu	0	30	45	135
70% Lu	9	20,9	45	135
80% Lu	6	24	45	135

Synthesis of β-$NaYF_4$:Yb,Er core particles

At room temperature, 12 ml of oleic acid, 12 ml of 1-octadecene and 24 ml of the hexane solution of the α-Na_xYF_{3+x}:Yb,Er precursor particles (12 mmol) were combined in a 100 ml three neck round bottom flask. The flask was connected to a Schlenk-line and the hexane removed by applying vacuum at room temperature. After switching to nitrogen atmosphere, 12 ml of oleic acid and 12 ml of 1-octadecene were added. The flask was placed under vacuum again and heated at 100 °C for one hour. The reaction vessel was then backfilled with nitrogen, heated to 300°C and kept at this temperature until all α-Na_xYF_{3+x}:Yb,Er precursor particles had dissolved and the growth of the β-$NaYF_4$:Yb,Er particles was completed. The heating mantle was removed when all precursor particles had dissolved to avoid Ostwald ripening of the β-$NaYF_4$:Yb,Er particles, resulting in broadening of their size distribution. The appropriate heating time was determined in test runs using XRD measurements to determine the phase composition of the product (see table below). When the temperature was lower than 40 °C, the particles were precipitated by adding 50 ml of ethanol. The particles were collected by centrifugation, subsequently redispersed in 10 ml of hexane and again precipitated with 10 ml of ethanol. This precipitate was finally redispersed in 24 ml of hexane and the solution stored in a refrigerator.

$NaYF_4$:Yb,Er	α-$NaREF_4$ / mmol	Conversion to β /min
20% Yb, 2% Er	12	95
40% Yb, 2% Er	12	95
60% Yb, 2% Er	12	80
98% Yb, 2% Er	12	60
60% Yb, 10% Er	12	110

Synthesis of β-$NaYF_4$:Yb,Er/$NaYF_4$:Lu core/shell particles

For the synthesis of core/shell particles, β-$NaYF_4$:Yb,Er core particles and α-Na_xYF_{3+x}:Lu particles, serving as precursor for the shell, were combined in a molar ratio of 1 to 7. Thus, 2 ml of the hexane solution of the core particles (1.0 mmol of β-$NaYF_4$:Yb,Er) and 14 ml of the hexane solution of the shell material (7.0 mmol of α-Na_xYF_{3+x}:Lu) were combined with 8 mL oleic acid and 8 mL octadecene in a 100 ml vessel. The stirred mixture was then placed under vacuum at room temperature to remove the hexane. Next, the flask was backfilled with nitrogen, 8 ml of oleic acid and 8 ml of 1-octadecene were added, vacuum was applied again and the solution heated to 100 °C. After heating for one hour under vacuum, the atmosphere was switched back to nitrogen and the reaction vessel heated to 300°C. The solution was kept at this temperature until all α-Na_xYF_{3+x}:Lu precursor particles had dissolved and the growth of the β-$NaYF_4$:Yb,Er/$NaYF_4$:Lu core/shell particles was completed. The heating mantle was removed when all precursor particles had dissolved to avoid Ostwald ripening of the core/shell particles. The appropriate heating time was determined again in test runs (see table below).

After cooling to room temperature, the core/shell particles were isolated und purified as described above for the β-$NaYF_4$:Yb,Er core particles.

β-$NaYF_4$:Yb, Er core particles		α-$NaYF_4$:Lu shell precursor		Core/shell particles
Dopants / %	β-$NaREF_4$ / mmol	Dopant / %	α-$NaREF_4$ / mmol	Conversion time / min
20% Yb, 2% Er	1	22% Lu	7	120
40% Yb, 2% Er	1	42% Lu	7	180
60% Yb, 2% Er	1	62% Lu	7	65
98% Yb, 2% Er	1	100%Lu	7	65 to 80
60% Yb, 10% Er	1	70% Lu	7	125
60% Yb, 20% Er	1	80% Lu	7	125
60% Yb, 40% Er	1	100% Lu	7	125

Absolute measurement of upconversion quantum yields at different excitation power densities

The quantum yields of the upconversion emission (Φ_{UC}) were determined absolutely at different excitation power densities (*P*) with a calibrated custom designed integrating sphere setup previously reported. [1] The setup included a very stable 8 W 976 nm laser diode as excitation light source and two filter wheels with neutral density filters of known transmittance, both in the excitation channel for controlled attenuation of the excitation power density (*P*) in small steps. Another filter wheel with edge, band pass, and neutral density filters is placed in the detection channel to avoid detector saturation. Detection of the transmitted and emitted photons was done with a silicon CCD. The design and calibration of the setup, the beam profile characterization, and the measurement procedure were described in detail in a recent publication. [1]

In short: the wavelength- and polarization-dependent spectral responsivity *s*($_{em}$) of the integrating sphere-spectrograph-CCD ensemble (emission correction curve) of the integrating sphere setup was determined with a calibrated spectral radiance transfer standard (calibrated wavelength dependence of the *spectral radiance* ($L_\lambda(\lambda)$). For the determination of the spectral responsivity, the spectral radiant power of the calibrated lamp, placed in front of the integrating sphere was measured. Prerequisites for the calibration of a spectrograph-CCD array ensemble are defined grating positions for each part of the spectrum with the corresponding detection filter used for the subsequent measurements in place. *F* presents the integrated spectral fluorescence photon flux $q^f_{p,\lambda}(\lambda_{em})$ at the detector, see equation 1S, that is calculated from the dark-count corrected signal of the emission detector $I_u(\lambda_{em})$ multiplied with the photon energy hc_0/λ_{em} and divided by the instrument´s relative spectral responsivity $s(\lambda_{em})$.

$$F = \int_{\lambda_{em1}}^{\lambda_{em2}} q^{f}_{p,\lambda}(\lambda_{em})d\lambda_{em} = (hc_0)^{-1} \int_{\lambda_{em1}}^{\lambda_{em2}} \frac{I_u(\lambda_{em})}{s(\lambda_{em})}\lambda_{em}d\lambda_{em} \qquad \text{(eq. 1S)}$$

P-dependent Φ_{UC} were calculated from the number of emitted photons (N_{em}) and the number of absorbed photons (N_{abs}) at the chosen excitation wavelength (see equation 2S) per integration time interval. N_{em} was obtained from the *P*-dependent flux of the upconverted photons by integration over all Er^{3+} emission bands between 370 nm and 890 nm. N_{abs} was derived from transmission measurements of the sample and a non-emissive blank, as also previously described. [1] [12]

$$\phi_{UC}(P) = N_{em}/N_{abs}, \quad \text{for } \lambda_{em} < \lambda_{abs} \qquad \text{(eq. 2S)}$$

For the determination of the relative intensity contributions of the red emission ($^4F_{9/2} \rightarrow {}^4I_{15/2}$, 635-658 nm), green emission ($^2H_{11/2}$ and $^4S_{3/2} \rightarrow {}^4I_{15/2}$, 510-570 nm), NIR emission at 810 nm ($^4I_{9/2} \rightarrow {}^4I_{15/2}$, 783-833 nm) and 845 nm ($^4S_{3/2} \rightarrow {}^4I_{13/2}$, 833-860 nm), and blue emission ($^2H_{9/2} \rightarrow {}^4I_{15/2,}$ 635-658 nm) were considered.

Additional Figures:

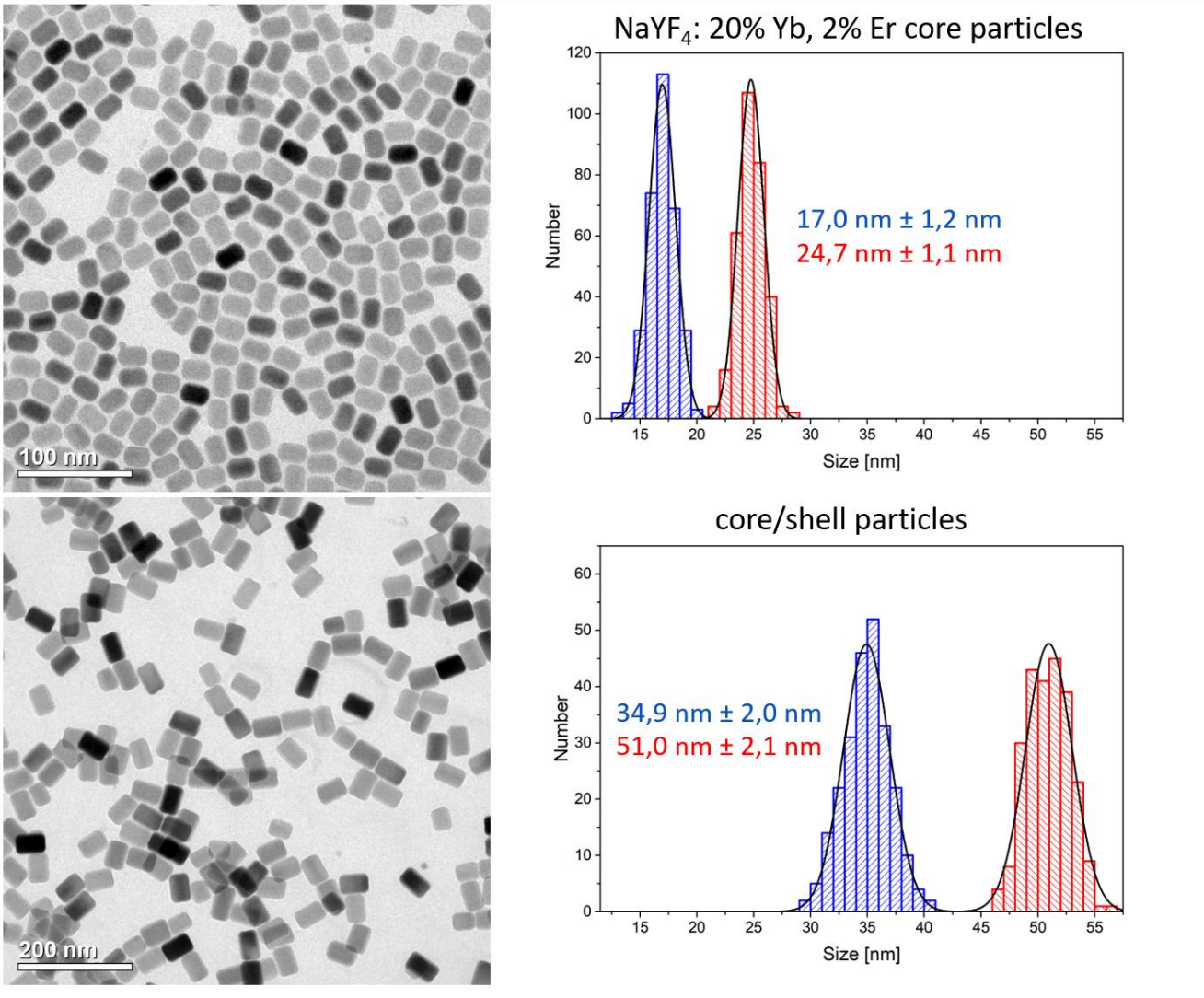

Figure S1 TEM image (left) and particle size histogram (right) of β-$NaYF_4$:20%Er,2%Er core particles (upper panel) and of β- $NaYF_4$:20%Er,2%Er/$NaYF_4$:22%Lu core/shell particles (lower panel). Particle length (red) and particle width (blue) are given separately in the histograms and were deduced from several TEM images. The shell increases the particle size by approximately a factor of two, since the core particles and the shell precursor were combined in a molar ratio of 1 to 7. Note the different scale bars in the TEM images.

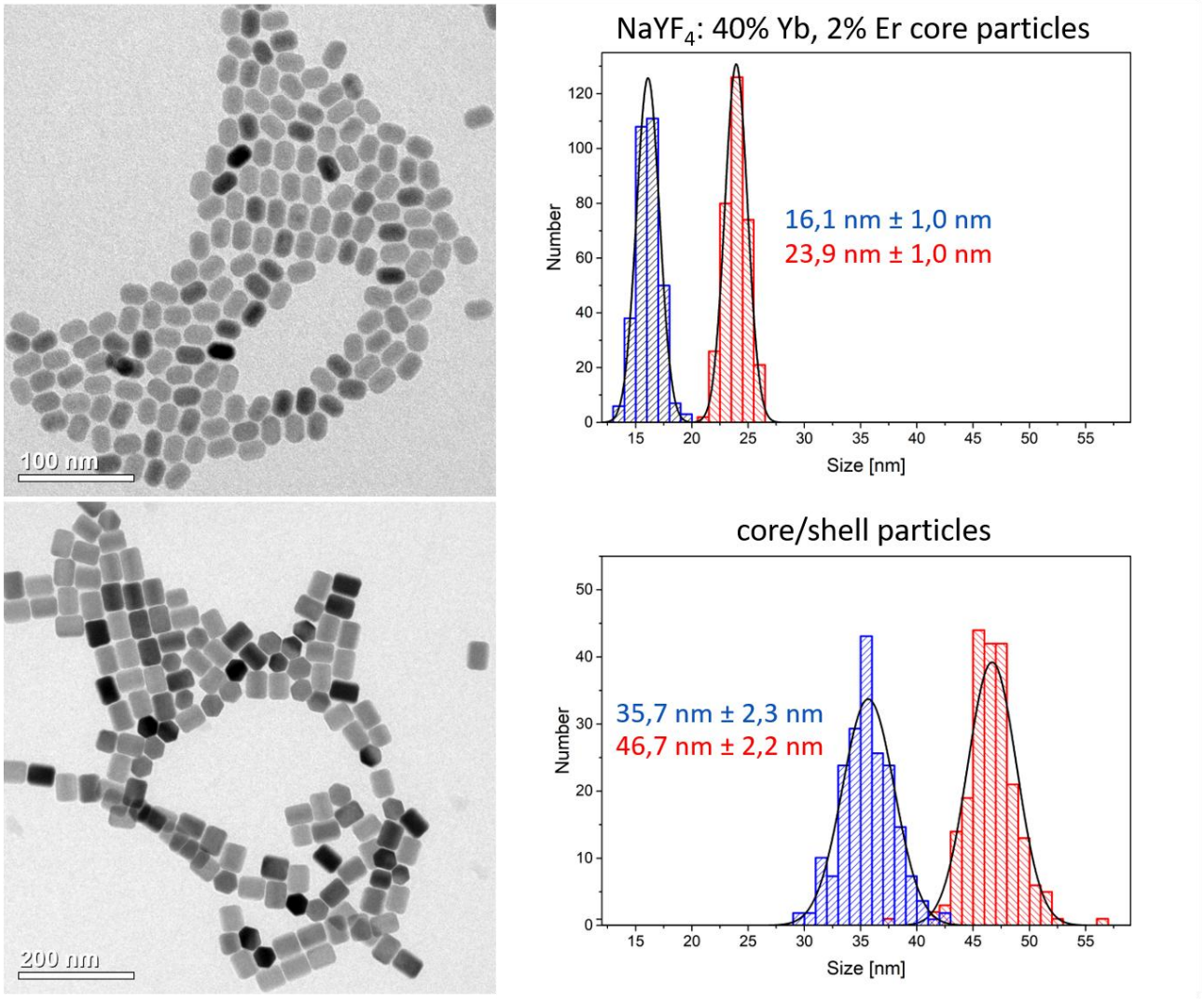

Figure S2 TEM image (left) and particle size histogram (right) of β-$NaYF_4$:40%Yb,2%Er core particles (upper panel) and of β-$NaYF_4$:40%Yb,2%Er/$NaYF_4$:42%Lu core/shell particles (lower panel). Particle length (red) and particle width (blue) are given separately in the histograms and were deduced from several TEM images. The shell increases the particle size by approximately a factor of two, since the core particles and the shell precursor were combined in a molar ratio of 1 to 7. Note the different scale bars in the TEM images.

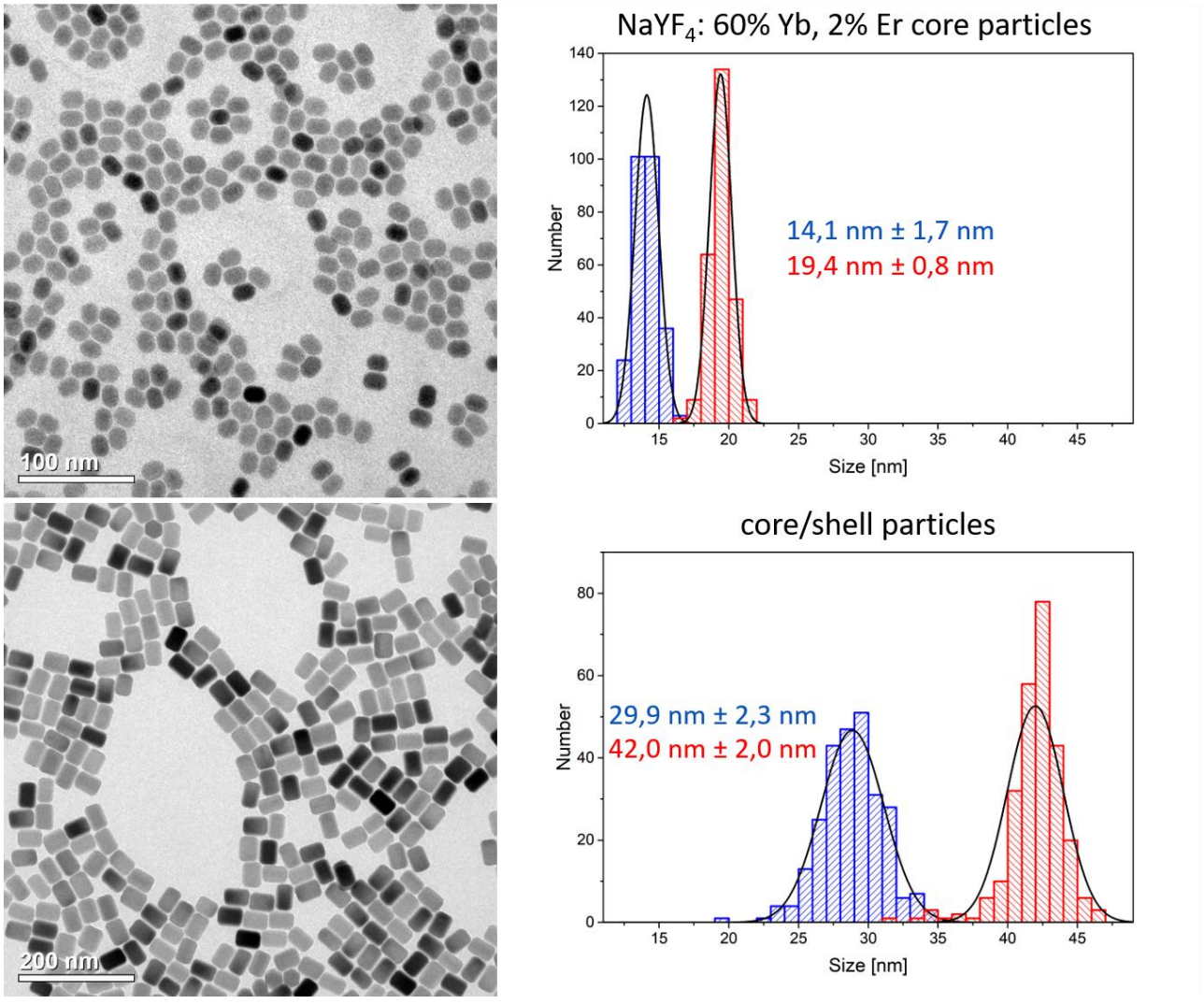

Figure S3 TEM image (left) and particle size histogram (right) of β- $NaYF_4$:60%Yb,2%Er core particles (upper panel) and of β- $NaYF_4$:60%Yb,2%Er/$NaYF_4$:62%Lu core/shell particles (lower panel). Particle length (red) and particle width (blue) are given separately in the histograms and were deduced from several TEM images. The shell increases the particle size by approximately a factor of two, since the core particles and the shell precursor were combined in a molar ratio of 1 to 7. Note the different scale bars in the TEM images.

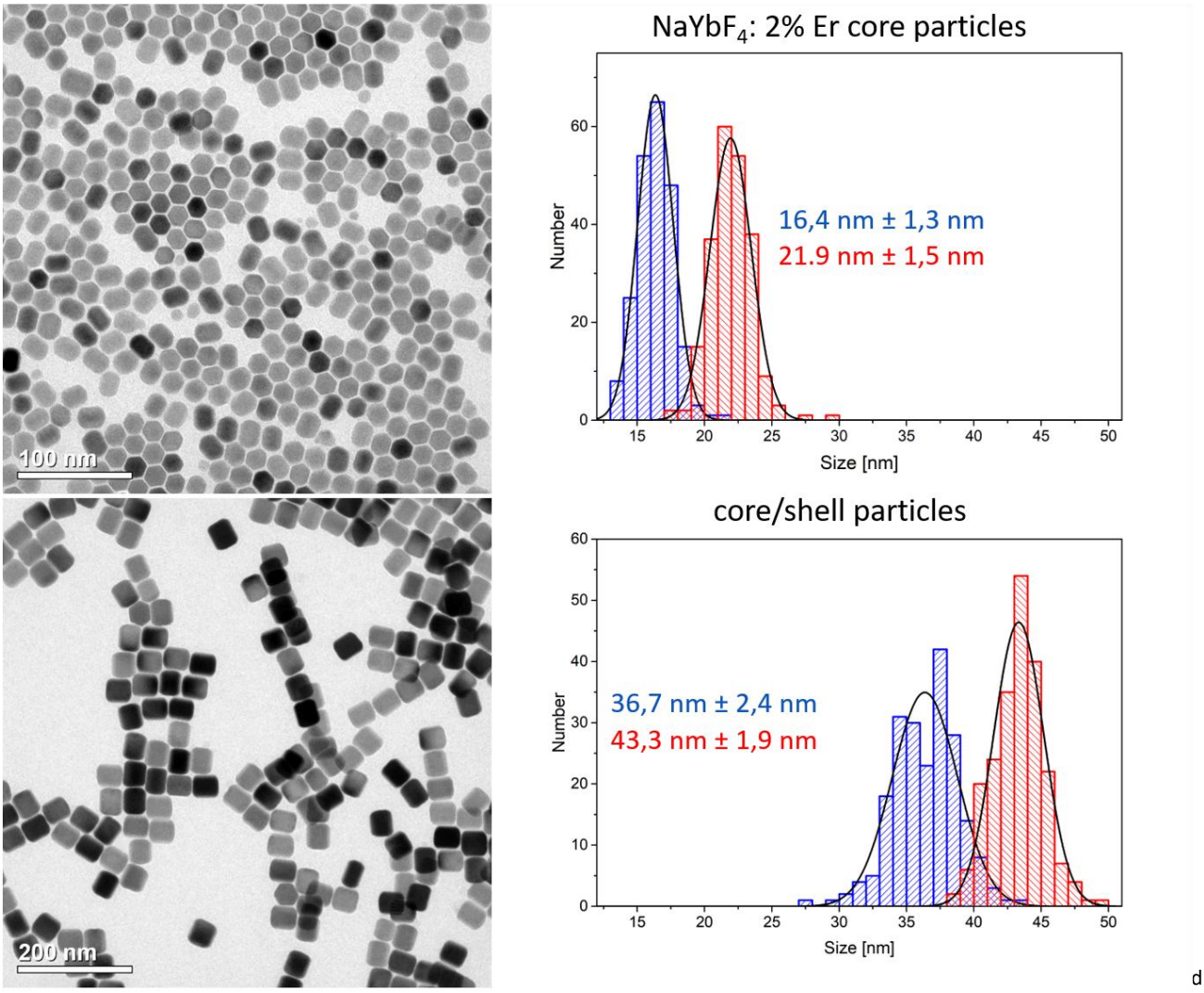

d of β- $NaYbF_4$:2%Er/$NaLuF_4$ core/shell particles (lower panel). Particle length (red) and particle width (blue) are given separately in the histograms and were deduced from several TEM images. The shell increases the particle size by approximately a factor of two, since the core particles and the shell precursor were combined in a molar ratio of 1 to 7. Note the different scale bars in the TEM images.

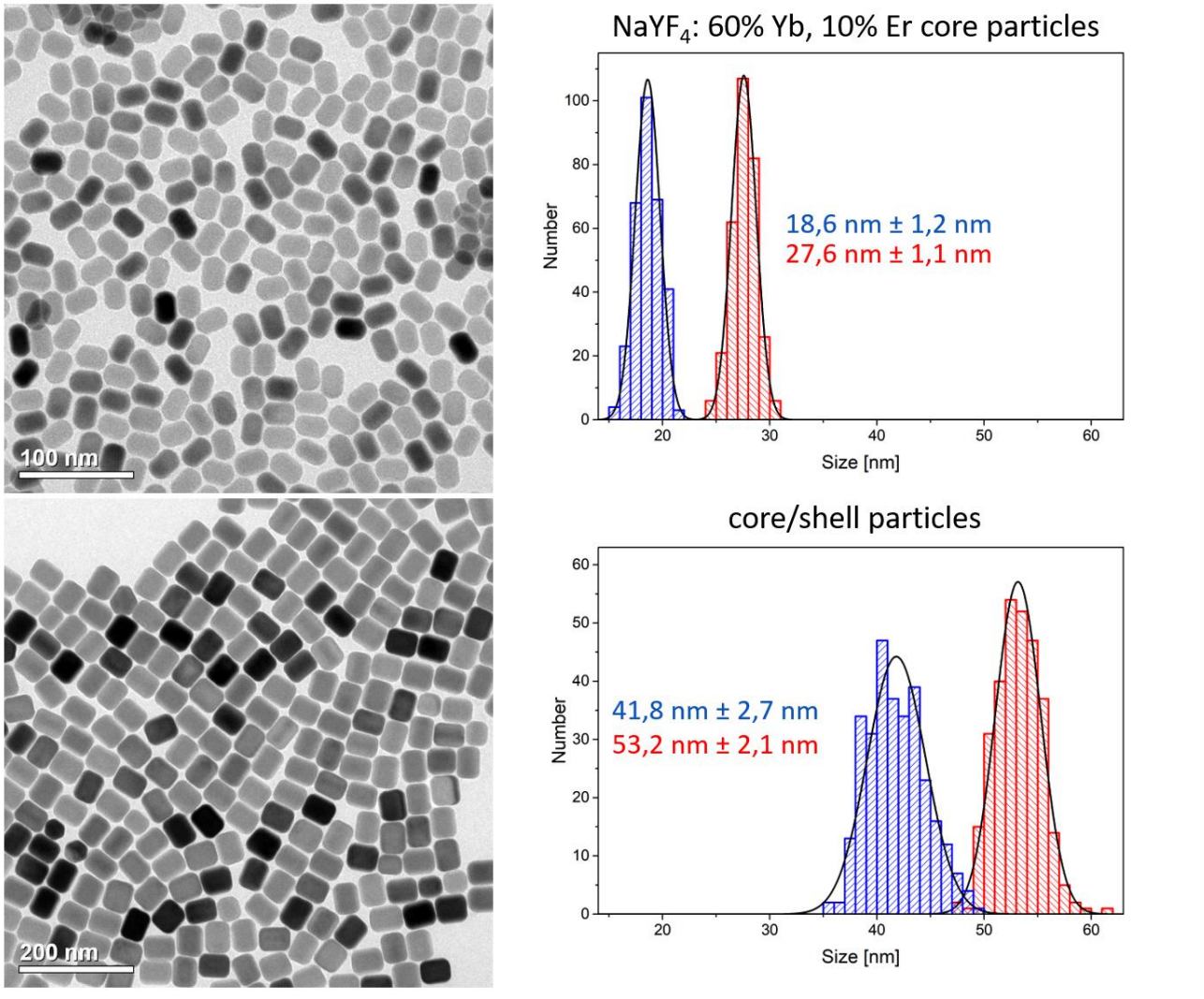

Figure S5 TEM image (left) and particle size histogram (right) of β-$NaYF_4$:60%Yb,10%Er core particles (upper panel) and of β-$NaYF_4$:60%Yb,10%Er /$NaYF_4$:70%Lu core/shell particles (lower panel). Particle length (red) and particle width (blue) are given separately in the histograms and were deduced from several TEM images. The shell increases the particle size by approximately a factor of two, since the core particles and the shell precursor were combined in a molar ratio of 1 to 7. Note the different scale bars in the TEM images.

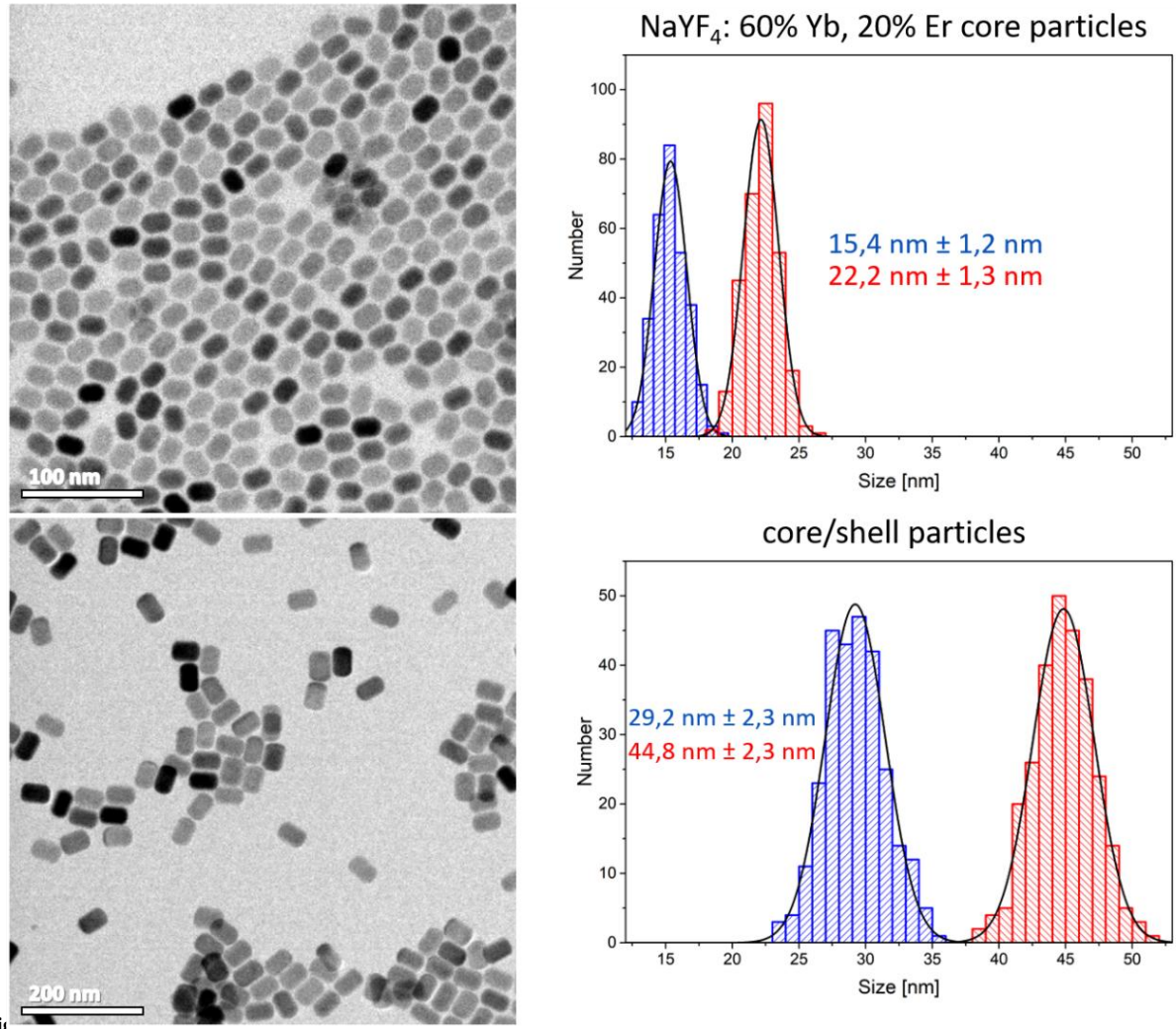

Figure 3 TEM image (left) and particle size histogram (right) of β-$NaYF_4$:60%Yb,20%Er core particles (upper panel) and of β-$NaYF_4$:60%Yb,20%Er/$NaYF_4$:80%Lu core/shell particles (lower panel). Particle length (red) and particle width (blue) are given separately in the histograms and were deduced from several TEM images. The shell increases the particle size by approximately a factor of two, since the core particles and the shell precursor were combined in a molar ratio of 1 to 7. Note the different scale bars in the TEM images.

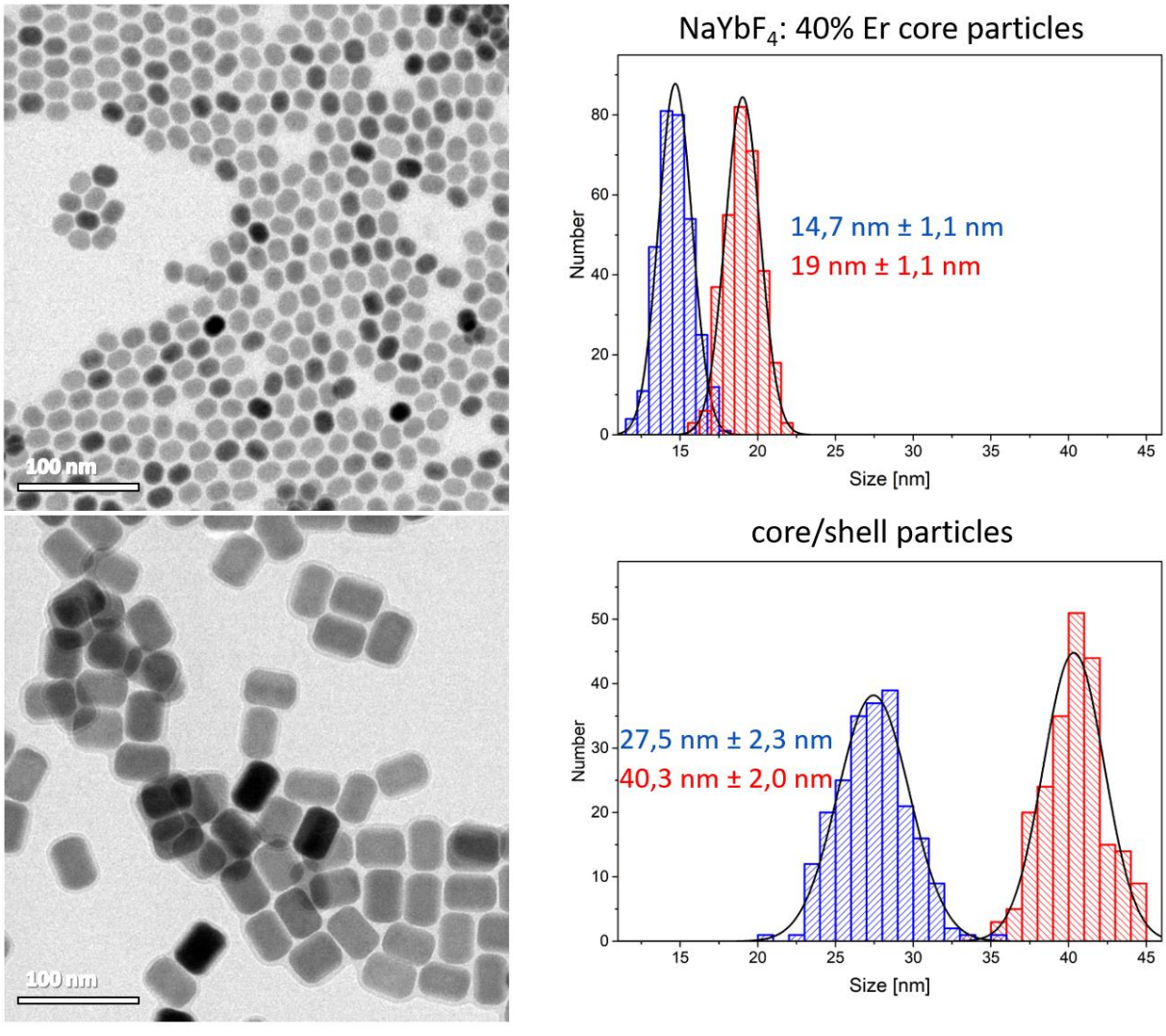

Figure S7 TEM image (left) and particle size histogram (right) of β-$NaYbF_4$:40%Er core particles (upper panel) and of β-$NaYbF_4$:40%Yb/$NaLuF_4$ core/shell particles (lower panel). Particle length (red) and particle width (blue) are given separately in the histograms and were deduced from several TEM images. The shell increases the particle size by approximately a factor of two, since the core particles and the shell precursor were combined in a molar ratio of 1 to 7.

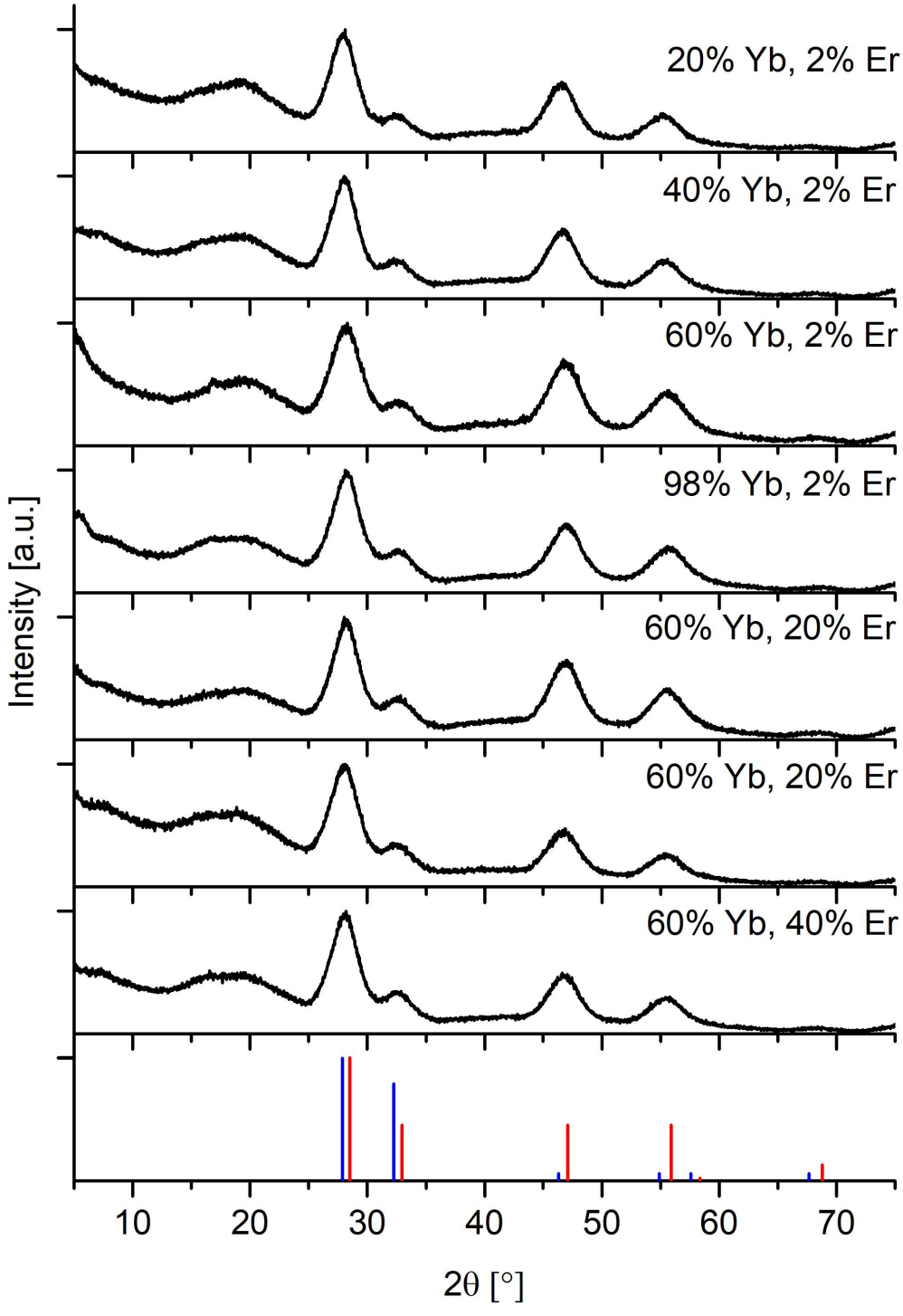

Figure S8 X-ray powder diffraction data (XRD) of cubic α- Na_xYF_{3+x}:Yb, Er particles used as precursors for the synthesis of hexagonal β- $NaYF_4$:Yb,Er core particles. Reference data for the cubic phase of $NaYF_4$ (PDF-No.: 00-027-1428) and the cubic phase of $NaYbF_4$ (PDF-No.: 00-27-1426) are given as blue and red lines, respectively.

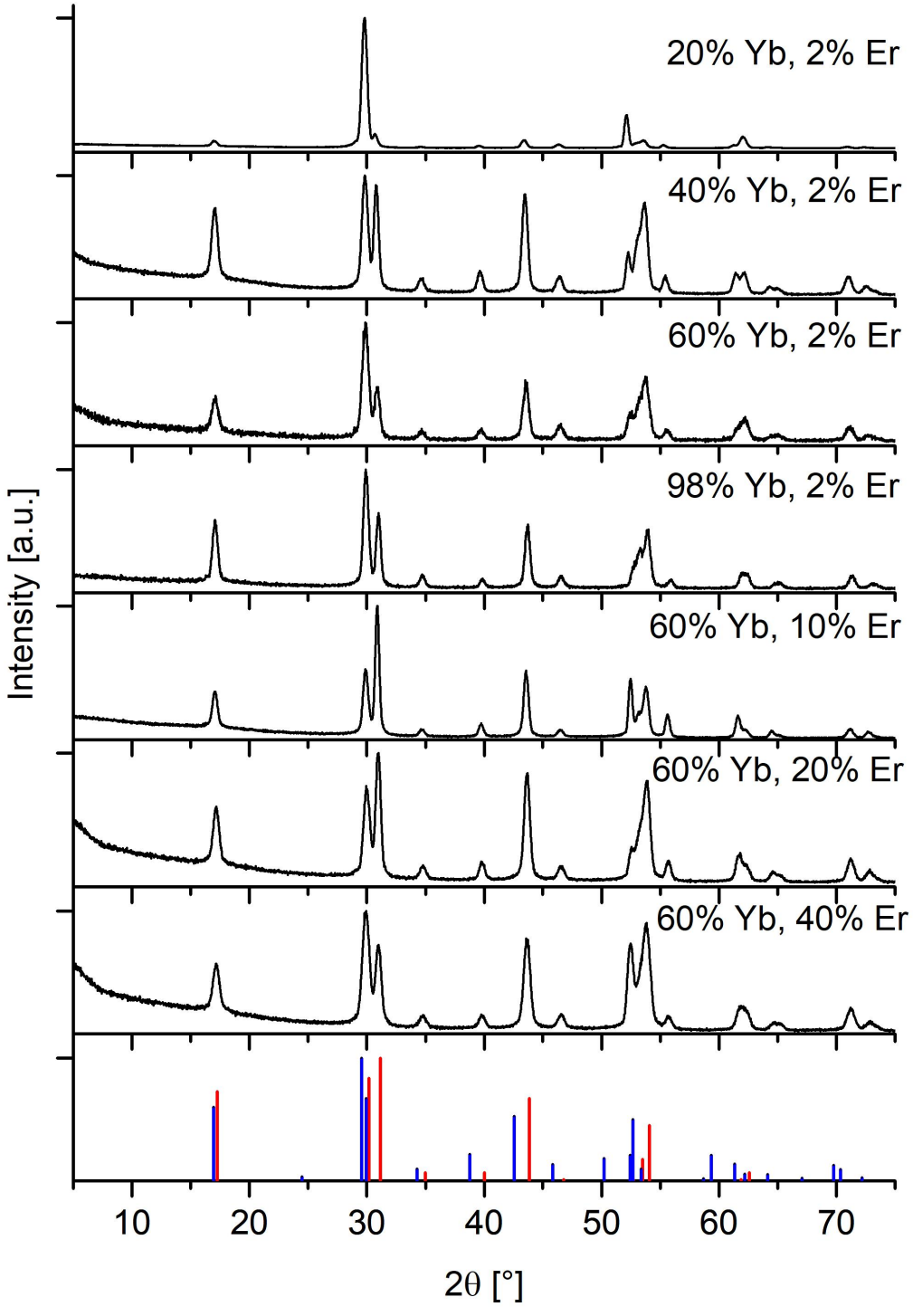

Figure S9 X-ray powder diffraction data (XRD) of the β- $NaYF_4$:Yb,Er core particles. High concentrations of Yb^{3+}/Er^{3+} results in a slight shift of the diffraction peaks to higher 2θ values as shown by the reference data for the hexagonal phase of $NaYF_4$ (blue, PDF-No.: 00-016-0334) and the hexagonal phase of $NaYbF_4$ (red, PDF-No.: 00-27-1427).

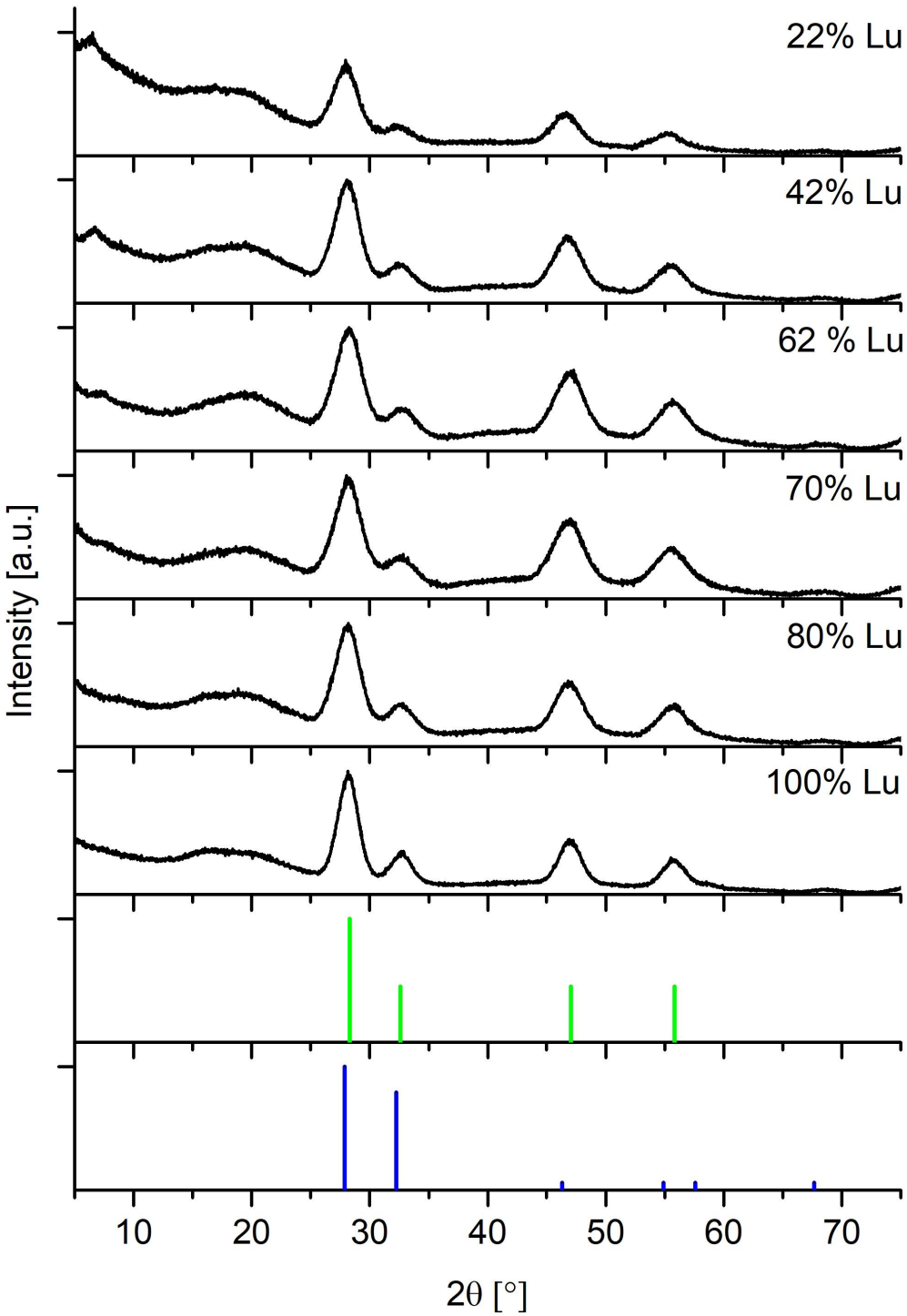

Figure S10 X-ray powder diffraction data (XRD) of cubic α- Na_xYF_{3+x}:Lu particles used as shell precursors. Reference data for the cubic phase of $NaYF_4$ (PDF-No.: 00-027-1428) and the cubic phase of $NaLuF_4$ (PDF-No.: 00-027-0725) are given as blue and green lines, respectively.

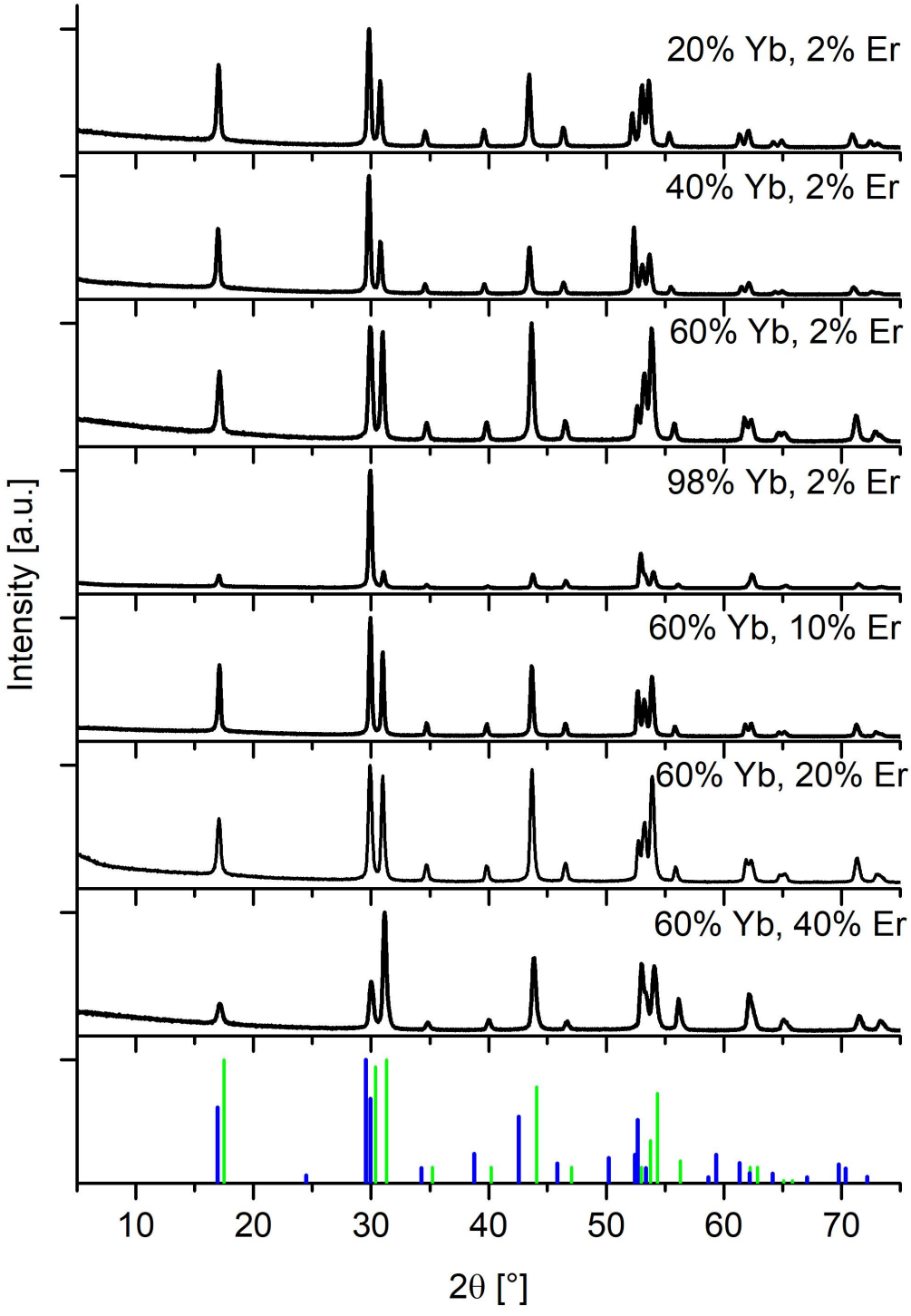

Figure S11 X-ray powder diffraction data (XRD) of the β- $NaYF_4$:Yb,Er/$NaYF_4$:Lu core/shell particles. High concentrations of Yb^{3+}, Er^{3+} and Lu^{3+} results in a slight shift of the diffraction peaks to higher 2θ values as shown by the reference data for the hexagonal phase of $NaYF_4$ (blue, PDF-No.: 00-016-0334) and the hexagonal phase of $NaLuF_4$ (green, PDF-No.: 00-27-0726).

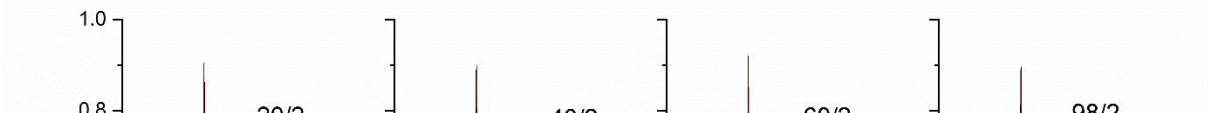

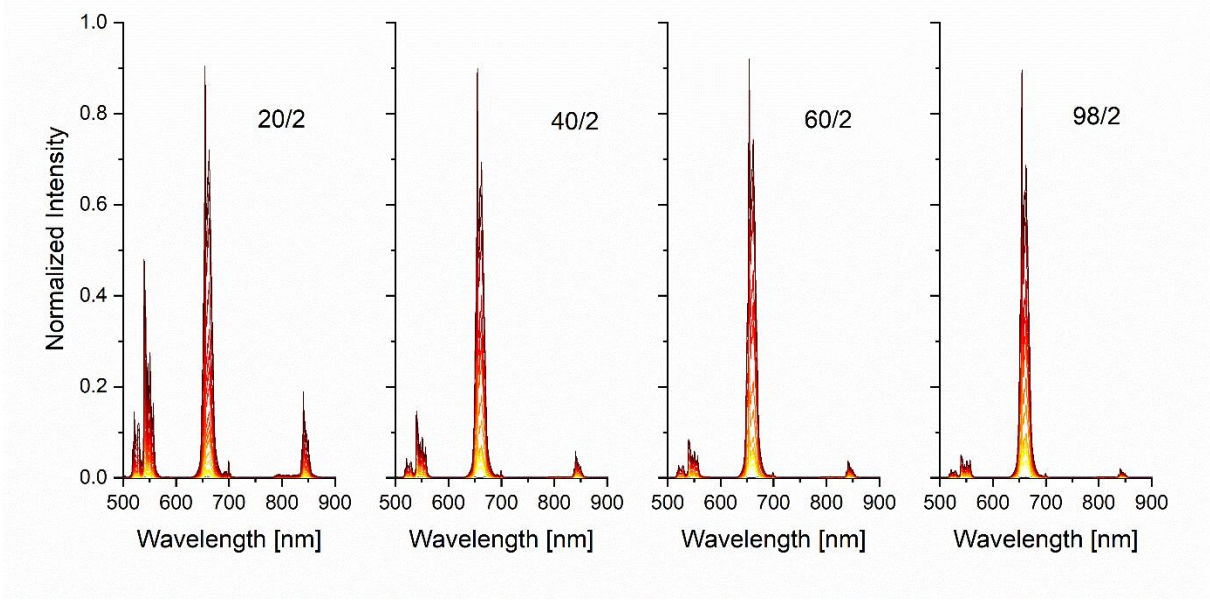

Figure S12 Excitation power dependent emission spectra of the Yb^{3+} concentration series, the Yb/Er ratio is indicated. The color code represents the increasing excitation powers via yellow -> black.

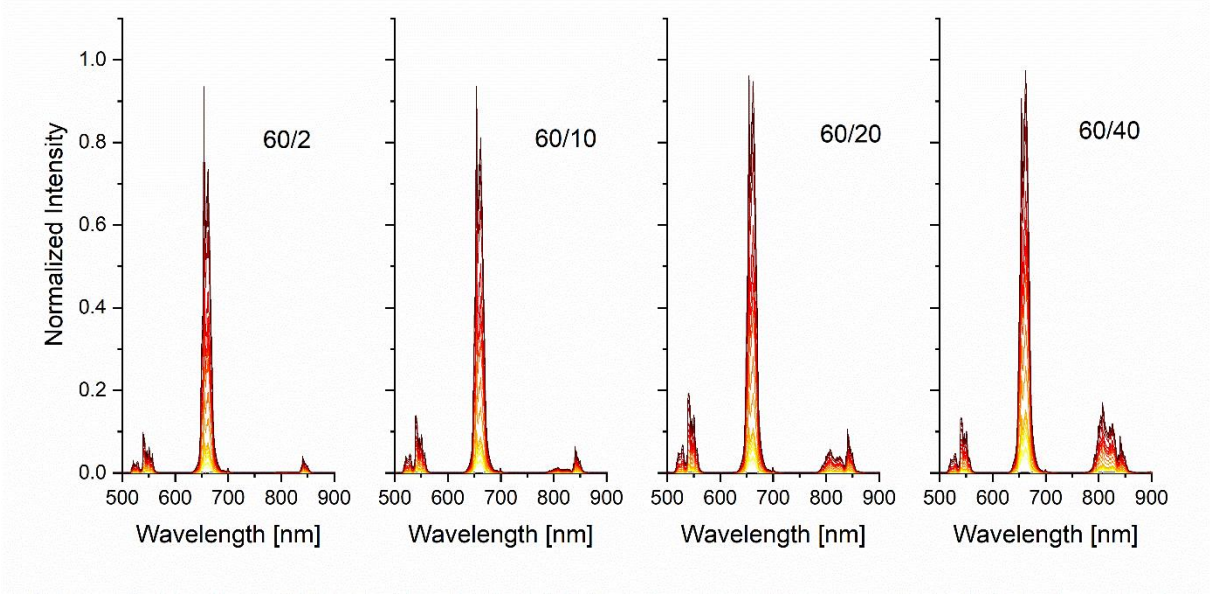

Figure S13 Excitation power dependent emission spectra of the Er^{3+} concentration series, the Yb/Er ratio is indicated. The color code represents the increasing excitation powers via yellow -> black.

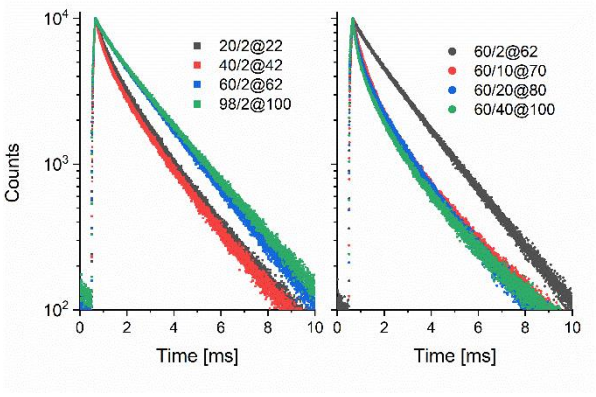

Figure S14 Luminescence decays of β-$NaYF_4$:Yb,Er/$NaYF_4$ core/shell particles. a) Particles doped with 2% Er^{3+} and 20 % (black), 40 % (red), 60 % (blue), and 98 % (green) of Yb^{3+}, respectively. b) Particles doped with 60% Yb^{3+} and 2 % (black), 10 % (red), 20 % (blue), and 40 % (green) of Er^{3+}, respectively. The long luminescence lifetime of the Yb^{3+} emission indicates a good shielding of the particle core in all cases. Excitation was at 978 nm and the Yb^{3+} emission was recorded at 1000 nm.

Literature

[1] C. Homann, L. Krukewitt, F. Frenzel, B. Grauel, C. Würth, U. Resch-Genger, M. Haase, *Angewandte Chemie Int. Ed.* **2018**, *57*, 8765-8769

[2] T. Rinkel, J.Nordmann, A. Naduviledathu Raj, M. Haase; *Nanoscale* **2014**, 6 (23), 14523 – 14530

[3] T. Rinkel, A. N. Raj, S. Dühnen, M. Haase, *Angewandte Chemie Int. Ed.* **2016**, *55*, 1164-1167

[4] S. Mondini, A. M. Ferretti, A. Puglisi, A. Ponti, *Nanoscale* **2012**, *4*, 5356-5372

[5] a) J. Rodríguez-Carvajal, *Laboratoire Leon Brillouin* **2001**; b) X. Cui, Z. Feng, Y. Jin, Y. Cao, D. Deng, H. Chu, S. Cao, C. Dong, J. Zhang, *Journal of Applied Crystallography* **2015**, *48*, 1581-1586

[6] M. Kaiser, C. Würth, M. Kraft, I. Hyppänen, T. Soukka, U. Resch-Genger, *Nanoscale* **2017**, *9*, 10051-10058